Dynamics of a Raman coupled model interacting with two quantized cavity fields

Christopher C. Gerry* and J. H. Eberly
Department of Physics and Astronomy, University of Rochester, Rochester, New York 14627
(Received 5 July 1990)

We describe the dynamics of an exactly solvable Raman coupled model interacting with two modes of a quantized cavity electromagnetic field. The model consists of a three-level atom in the Λ configuration whose excited state is considered to be far off resonance and is adiabatically eliminated. The effective Hamiltonian for this system contains products of the transition operators between the two ground-state levels and a field annihilation operator from one mode and a creation operator from the other. This Hamiltonian provides an example of a zero-photon process. We study the atomic inversion and investigate the production of nonclassical effects such as antibunched light, violations of the Cauchy-Schwartz inequality, and squeezing.

I. INTRODUCTION

Over the last decade there has been much activity in the theoretical[1] and experimental[2] study of simple nontrivial models of quantum-optical interactions involving one atom with a few energy levels and one or more near resonant modes of the quantized electromagnetic field. The prototype of such systems is the well-known Jaynes-Cummings model[3] in which a single-mode field interacts with a two-level atom. When the rotating-wave approximation is used this model is exactly solvable. A number of quantum effects having no classical analog have been discovered in the dynamics of this model even when the field is assumed to be initially in a coherent state. These include the collapse and revival of the Rabi oscillation of the atomic inversion and of the atomic dipole moment,[4] vacuum-field Rabi oscillations,[5] and the production of novel states of radiation.[6] Multiphoton versions of the Jaynes-Cummings models have also been much studied[7–11] and micromasers operating on one-photon and two-photon transitions have been realized in the laboratory.[12] Jaynes-Cummings-like models having three or more levels interacting with one or more modes of the cavity field have also been extensively studied,[1,13] where phenomena similar to that seen in the two-level, one-mode case are also observed.

In most studies of the Jaynes-Cummings model, the basic processes involve either a net loss or gain of photons. In the present work we study, as an extension of the few-level systems in unusual environments already alluded to above, a model system for which the net gain or loss of photons is zero—a zero-photon process. The particular model we have in mind consists of a three-level atom in the Λ configuration interacting with two modes of the field under the assumption of exact two-photon resonance, as shown in Fig. 1. Level 2 is assumed to be far off resonance and will be adiabatically removed so that this excited level acts only as a virtual state in transitions between levels 1 and 3. The resulting model therefore consists of two nondegenerate "ground" states connected by a zero-photon process where a photon absorbed in one mode is emitted in the other, with the atom making transitions through the virtual state. The essential difference between the discussions of the three-level system of Fig. 1 by Yoo and Eberly[1] and in this paper is that in the former, the second level participates significantly in the population dynamics. In the present case the model may be interpreted as a cavity version of Raman scattering in which mode 1 is the pump field, mode 2 is the Stokes field, and no anti-Stokes field is present (due to lack of a cavity resonance). For this reason we refer to our model as the two-mode Raman coupled model. After the adiabatic elimination of the second level, the effective interaction Hamiltonian has the form of the usual Jaynes-Cummings model but with the single-mode field operators replaced by products of an annihilation operator of one mode and a creation operator of the other. The techniques normally used to solve the Jaynes-Cummings model[1,14] may also be used in the present case.

We should note here that a one-mode Raman coupled model involving a zero-photon process has already been discussed by Knight[15] and Phoenix and Knight[16] in connection with the collapse and revival of the Rabi oscillations. In their model, two degenerate atomic states are connected by a single-mode two-photon coupling. Unlike the usual Jaynes-Cummings model, in that case the atom-

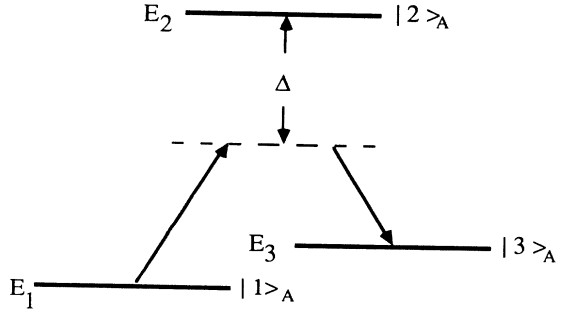

FIG. 1. Energy-level diagram of the three-level atom in the Λ configuration. The detuning Δ is large compared to $E_3 - E_1$.

ic inversion can be summed in closed form and exhibits regular and complete revivals. Obviously, the Knight-Phoenix model is closely related to Ref. 1 and to the model presently under investigation, but many results are strikingly different.

This paper is organized as follows. In Sec. II we identify the important parameters of our model and give its effective Hamiltonian. Expressions for the density matrix elements for the field and atomic dynamics are derived. In Sec. III we discuss the atomic dynamics, in particular the atomic inversion between the first and third levels, assuming both modes initially in coherent states or with the pump mode in a coherent state and the Stokes mode in the vacuum. We take the atom to be initially in the state $|1\rangle_A$. The dynamical evolution is essentially symmetric, as we show, with respect to the states $|1\rangle_A$ and $|3\rangle_A$. In Sec. IV we study the dynamics of the field, paying particular attention to the possibility that nonclassical states might be generated by the interaction. Specifically we investigate the possible appearance of sub-Poisson statistics (actually photon antibunching) in each mode, anticorrelations between the modes, violation of the Cauchy-Schwartz inequality, and the appearance of squeezing. Section V concludes the paper with a brief summary and some discussion. An Appendix is included wherein the effective Hamiltonian of our system is derived by adiabatic elimination of the state $|2\rangle_A$.

II. MODEL AND SYSTEM DYNAMICS

The energy-level configuration of our model is given in Fig. 1 where E_1, E_2, and E_3 are the energies of levels 1, 2, and 3, respectively. We assume that $E_3 > E_1$ and that $E_2 \gg E_1, E_3$. The Hamiltonian describing this system is given by

$$H = H_0 + H_I \tag{2.1}$$

where

$$H_0 = E_1\sigma_{11} + E_2\sigma_{22} + E_3\sigma_{33} + \hbar\omega_1 a_1^\dagger a_1 + \hbar\omega_2 a_2^\dagger a_2 \tag{2.2a}$$

is the free atom plus free field Hamiltonian and

$$H_I = \hbar g_{12}(a_1\sigma_{21} + \sigma_{12}a_1^\dagger) + \hbar g_{23}(a_2\sigma_{23} + \sigma_{32}a_2^\dagger) \tag{2.2b}$$

is the interaction Hamiltonian. The symbols a_i $(i=1,2)$ represent the field operators of modes 1 and 2 while the σ_{ij} $(i,j=1,2,3)$ are operators in the atom subspace, σ_{ii} being the level occupation numbers and σ_{ij} $(i \neq j)$ being the transition operators from levels j to i. We shall designate mode 1 of frequency ω_1 as the pump mode and mode 2 of frequency ω_2 as the Stokes mode, and we assume $\omega_2 < \omega_1$. The interaction Hamiltonian (2.2b) couples the pump mode to the first and second levels while the Stokes mode is coupled only between the second and third where g_{12} and g_{23} are the respective dipole coupling constants and are assumed real. We assume that the cavity is tuned consistent with two-photon energy conservation $(E_3 - E_1 = \hbar\omega_1 - \hbar\omega_2)$ so that there is only one detuning parameter, namely Δ, defined by

$$\hbar\Delta = E_2 - E_1 - \hbar\omega_1 = E_2 - E_3 - \hbar\omega_2 , \tag{2.3}$$

which we shall assume to be large, i.e., $\hbar\Delta \gg E_3 - E_1$. The adiabatic removal of the second level, as described in the Appendix, results in the effective interaction Hamiltonian

$$H_{I,\text{eff}} = -\hbar\lambda(\sigma_+ a_1 a_2^\dagger + \sigma_- a_1^\dagger a_2) \tag{2.4}$$

where $\sigma_+ = \sigma_{31}$ and $\sigma_- = \sigma_{13}$ are the effective atomic raising and lowering operators between levels 1 and 3 and λ is the effective coupling constant given by $\lambda = 2g_{12}g_{23}/\Delta$. Since we are assuming the second level to be very far off resonance, we set the occupation of that state to zero, i.e., $\sigma_{22} = 0$. Thus we have $\sigma_{11} + \sigma_{33} = 1$ and we can rewrite the free Hamiltonian is

$$H_0 = \frac{\hbar}{2}\omega_0\sigma_0 + \hbar\omega_1 a_1^\dagger a_1 + \hbar\omega_2 a_2^\dagger a_2 + (E_1 + E_3)I \tag{2.5}$$

where $\hbar\omega_0 \equiv E_3 - E_1 = \hbar(\omega_1 - \omega_2)$ and $\sigma_0 = \sigma_{33} - \sigma_{11}$.

Since the energy is conserved during the transition, H_0 itself is a constant of the motion and therefore

$$[H_0, H_{I,\text{eff}}] = 0 . \tag{2.6}$$

Another constant of the motion is the total photon number $N = a_1^\dagger a_1 + a_2^\dagger a_2$, which is constant as a direct consequence of the fact that we are dealing with a zero-photon process.

The bare states of our system will be denoted as $|i; n_1 n_2\rangle \equiv |i\rangle_A \otimes |n_1, n_2\rangle_F$, where $i = 1,3$ is the atomic label and $|n_1, n_2\rangle_F \equiv |n_1\rangle \otimes |n_2\rangle$ is a direct product field state for modes 1 and 2.

To obtain the system dynamics we use the density operator formalism. The density operator for the atom-field system is $\rho(t)$, and it evolves according to

$$\rho(t) = U(t)\rho(0)U^\dagger(t) . \tag{2.7}$$

But because of Eq. (2.6), the evolution operator factors as

$$U(t) = U_0(t)U_I(t) \tag{2.8}$$

where

$$U_0(t) = \exp(-iH_0 t/\hbar) \tag{2.9a}$$

and

$$U_I(t) = \exp(-iH_{I,\text{eff}} t/\hbar) . \tag{2.9b}$$

Thus we may write

$$\rho(t) = U_0(t)\rho_I(t)U_0^\dagger(t) \tag{2.10}$$

where

$$\rho_I(t) = U_1(t)\rho(0)U_I^\dagger(t) . \tag{2.11}$$

Here $\rho_I(t)$ is, of course, just the density operator in the interaction picture where the system is driven by $H_{I,\text{eff}}$ which contains all the essential dynamics. The operator $U_0(t)$ merely contributes a phase factor in each atomic subspace. For any Schrödinger operator O_s, we have

$$\begin{aligned}\langle O(t)\rangle &= \text{Tr}[\rho(t)O_s] \\ &= \text{Tr}[\rho_I(t)O_I(t)]\end{aligned} \tag{2.12}$$

where

$$O_I(t)=U_0^{\dagger}(t)O_s U_0(t) . \tag{2.13}$$

In what follows, all field quantities will be evaluated in the interaction picture.

In order to explore the dynamics of the atom and of the field we introduce reduced atomic and field density operators, $\rho^A(t)$ and $\rho^F(t)$, respectively, whose matrix elements are given by

$$\rho_{ij}^A(t)=\sum_{n_1=0}^{\infty}\sum_{n_2=0}^{\infty}\langle i;n_1n_2|\rho(t)|j;n_1n_2\rangle , \tag{2.14}$$

$$\rho^F\begin{Bmatrix}m_1 & n_1\\ m_2 & n_2\end{Bmatrix}(t)=\sum_{\substack{i=1\\ i\neq 2}}^{3}\langle i;m_1m_2|\rho(t)|i;n_1n_2\rangle . \tag{2.15}$$

For the atomic system only the inversion $W(t)=\rho_{I_{33}}^A(t)-\rho_{I_{11}}^A(t)$ will be investigated. Since $\rho_{I_{11}}^A(t)+\rho_{I_{33}}^A(t)=1$, this may be written as $W(t)=2\rho_{I_{33}}^A(t)-1$ or $W(t)=1-2\rho_{I_{11}}^A(t)$. Only the necessary atomic density matrix elements will be calculated. We assume that at time $t=0$ the density operator factors into its atomic and field parts

$$\rho(0)=\rho^A(0)\otimes\rho^F(0) . \tag{2.16}$$

We further assume that initially, the field modes are in coherent states $|\alpha_1,\alpha_2\rangle$ given by

$$|\alpha_1,\alpha_2\rangle=\sum_{n_1=0}^{\infty}\sum_{n_2=0}^{\infty}C_{n_1n_2}|n_1,n_2\rangle , \tag{2.17}$$

where

$$C_{n_1n_2}=\exp[-\tfrac{1}{2}(|\alpha_1|^2+|\alpha_2|^2)]\frac{\alpha_1^{n_1}\alpha_2^{n_2}}{\sqrt{n_1!n_2!}} , \tag{2.18}$$

so that $\rho^F(0)=|\alpha_1,\alpha_2\rangle\langle\alpha_1,\alpha_2|$. Now further assuming the atom to be initially in the ground state $|1\rangle_A$, then $\rho^A(0)=|1\rangle_{A\,A}\langle 1|$. Using standard procedures,[1,14] the following necessary matrix elements, in the interaction picture, may be obtained:

$$\rho_{I_{11}}^A(t)=\sum_{n_1=0}^{\infty}\sum_{n_2=0}^{\infty}|C_{n_1n_2}|^2\cos^2\{\lambda t[n_1(n_2+1)]^{1/2}\} , \tag{2.19a}$$

$$\rho_1^F\begin{Bmatrix}m_1 & n_1\\ m_2 & n_2\end{Bmatrix}(t)=C_{n_1n_2}C^*_{m_1m_2}\cos\{\lambda t[n_1(n_2+1)]\}^{1/2}\cos\{\lambda t[m_1(m_2+1)]^{1/2}\}$$
$$+C_{n_1+1,n_2-1}C^*_{m_1+1,m_2-1}\sin\{\lambda t[n_2(n_1+1)]^{1/2}\}\sin\{\lambda t[m_2(m_1+1)]^{1/2}\} . \tag{2.19b}$$

On the other hand if the atom is initially in state $|3\rangle_A$, with $\rho^A(0)=|3\rangle_{A\,A}\langle 3|$ we then have

$$\rho_{I_{33}}^A(t)=\sum_{n_1=0}^{\infty}\sum_{n_2=0}^{\infty}|C_{n_1n_2}|^2\cos^2\{\lambda t[n_2(n_1+1)]^{1/2}\} , \tag{2.20a}$$

$$\rho_1^F\begin{Bmatrix}m_1 & n_1\\ m_2 & n_2\end{Bmatrix}(t)=C_{n_1n_2}C^*_{m_1m_2}\cos\{\lambda t[n_2(n_1+1)]^{1/2}\}\cos\{\lambda t[m_2(m_1+1)]^{1/2}\}$$
$$+C_{n_1-1,n_2+1}C^*_{m_1-1,m_2+1}\sin\{\lambda t[n_1(n_2+1)]^{1/2}\}\sin\{\lambda t[m_1(m_2+1)]^{1/2}\} . \tag{2.20b}$$

As we have said before, we shall be interested only in the case when the atom is initially in state $|1\rangle_A$. There is no loss of generality here since the formulas in Eqs. (2.19) and (2.20) are symmetric under the double interchange $n_1\leftrightarrow n_2$ and $m_1\leftrightarrow m_2$.

III. ATOMIC INVERSION

We study the dynamics of the atomic inversion as a first example of nontrivial nonclassical behavior in this model. As discussed above, we need study only the case when the atom is deexcited initially. The atomic inversion is therefore, from Eq. (2.19a), given by

$$W(t)=1-2\rho_{I_{11}}^A(t)$$
$$=1-2\sum_{n_1=0}^{\infty}\sum_{n_2=0}^{\infty}|C_{n_1n_2}|^2\cos^2\{\lambda t[n_1(n_2+1)]^{1/2}\}$$
$$=-\sum_{n_1n_2}|C_{n_1n_2}|^2\cos(t\Omega_{n_1n_2}) \tag{3.1}$$

where

$$\Omega_{n_1n_2}=2\lambda[n_1(n_2+1)]^{1/2} \tag{3.2}$$

are quantum electrodynamic Rabi frequencies for our model. Also from Eq. (2.18) we have

$$|C_{n_1n_2}|^2=P_{n_1}(\bar{n}_1)P_{n_2}(\bar{n}_2) \tag{3.3}$$

where

$$P_{n_i}(\bar{n}_i)=e^{-\bar{n}_i}\frac{\bar{n}_i^{\,n_i}}{n_i!} \tag{3.4}$$

and where $\bar{n}_i=|\alpha_i|^2$ is the initial average photon number in the ith mode.

Let us now consider the special case when $\bar{n}_2=0$. We then have $|C_{n_1 n_2}|^2=P_{n_1}(\bar{n}_1)\delta_{n_2,0}$. The expression for the inversion therefore reduces to

$$W(t)=-\sum_{n_1} P(n_1)\cos(t\Omega_{n_1 0}) \tag{3.5}$$

where $\Omega_{n_1 0}=2\lambda(n_1)^{1/2}$. This is the series obtained for the inversion in the usual Jaynes-Cummings model, with zero detuning, driven by an initial coherent state and we expect to see the usual collapse and revival phenomena in the time record of the inversion. For later use we briefly review the standard analysis (see Ref. 4) that predicts the collapse time and the revival times. The collapse time t_c is estimated from the spread of Rabi frequencies that make significant contributions to the sum in Eq. (3.5). For $\bar{n}_1 \gg 1$, and with $\Delta n_1=\bar{n}_1^{\,1/2}$, t_c is estimated by

$$[\Omega(\bar{n}_1+\bar{n}_1^{\,1/2})-\Omega(\bar{n}_1-\bar{n}_1^{\,1/2})]t_c\sim 1 \tag{3.6}$$

where $\Omega(\bar{n}_1)=2\lambda(\bar{n}_1)^{1/2}$. For $\bar{n}_1^{\,1/2}\ll\bar{n}_1$, we obtain $t_c\sim\lambda^{-1}$. On the other hand, the interval between revivals T_R may be estimated as the time when two neighboring terms in Eq. (3.5) for $n\sim\bar{n}$ and $n\sim\bar{n}+1$ differ in phase by a factor of 2π. That is, T_R is estimated by

$$[\Omega(\bar{n}_1+1)-\Omega(\bar{n}_1)]T_R\cong 2\pi \tag{3.7}$$

from which we obtain

$$T_R=2\pi\lambda^{-1}\bar{n}_1^{\,1/2}\,. \tag{3.8}$$

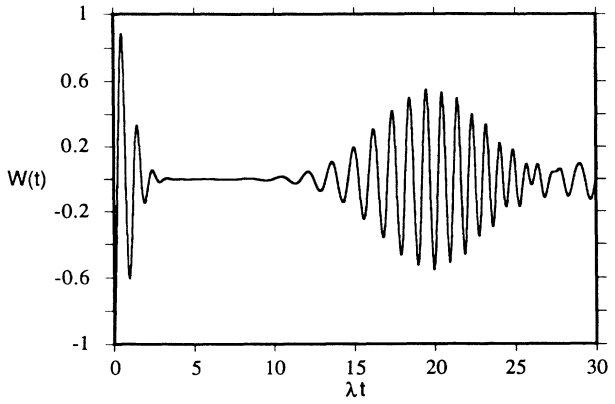

FIG. 2. Atomic inversion $W(t)$ vs the scaled time λt for $\bar{n}_1=10$, $\bar{n}_2=0$.

As a specific example, in Fig. 2, we plot the inversion $W(t)$ versus λt for $\bar{n}_1=10$ and $\bar{n}_2=0$. As expected, we see a time record resembling that for the usual Jaynes-Cummings model. The first revival occurs at $\lambda t\simeq 20$ as

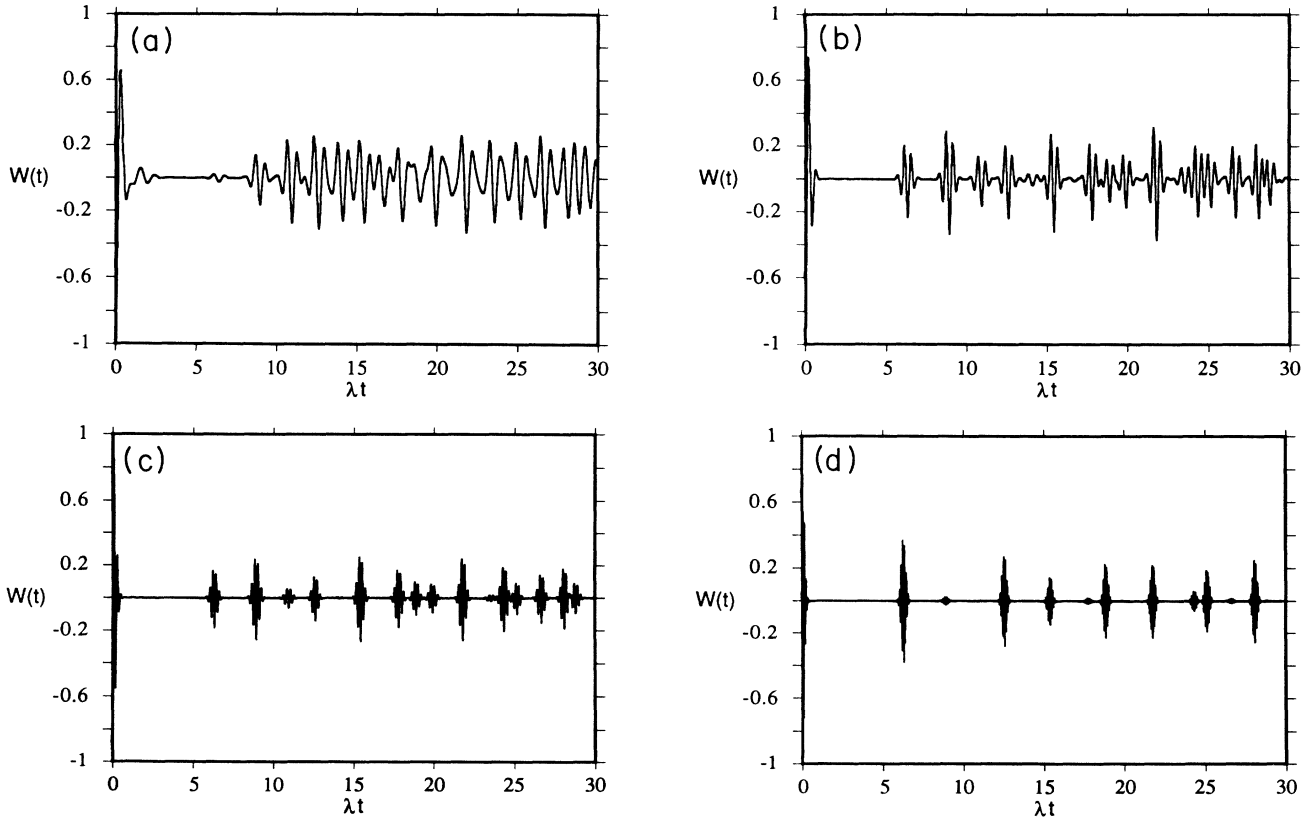

FIG. 3. Atomic inversions $W(t)$ vs the scaled time λt for various $\bar{n}_1,\bar{n}_2$. (a) $\bar{n}_1=10$, $\bar{n}_2=1.5$; (b) $\bar{n}_1=10$, $\bar{n}_2=5$; (c) $\bar{n}_1=20.5$, $\bar{n}_2=12.33$; (d) $\bar{n}_1=30$, $\bar{n}_2=30$.

predicted from Eq. (3.8).

For cases when $\bar{n}_2 \neq 0$, the revival patterns are quite different. They even present something of a puzzle which is not fully understood. In Fig. 3 we display several examples of the evolution of the atomic inversion for various $\bar{n}_1$ and $\bar{n}_2$. We immediately notice, in contrast to the usual case and in very strong contrast to the related zero-photon (but one-mode) case studied by Knight and Phoenix,[15,16] that the positions in time of the revivals are essentially independent of $\bar{n}_1$ and $\bar{n}_2$. This observation can be partially explained as follows. First we write Eq. (3.1) as

$$W(t) = -\mathrm{Re}\left[\sum_{n_1=0}^{\infty} \sum_{n_2=0}^{\infty} P_{n_1}(\bar{n}_1) P_{n_2}(\bar{n}_2) \times e^{2i\lambda t[n_1(n_2+1)]^{1/2}} \right] . \tag{3.9}$$

The rapid oscillation in the time record is just the dominant Rabi oscillation which occurs for $n_1 = \bar{n}_1$ and $n_2 = \bar{n}_2$, i.e., $\Omega(\bar{n}_1, \bar{n}_2) = 2\lambda[\bar{n}_1(\bar{n}_2+1)]^{1/2}$. We now Taylor expand the frequencies $2\lambda[n_1(n_2+1)]^{1/2}$ about $\bar{n}_1$ and $\bar{n}_2$ to obtain

$$\begin{aligned} 2\lambda[n_1(n_2+1)]^{1/2} = {} & 2\lambda[\bar{n}_1(\bar{n}_2+1)]^{1/2} + \lambda \left[\frac{\bar{n}_2+1}{\bar{n}_1} \right]^{1/2} (n_1-\bar{n}_1) + \lambda \left[\frac{\bar{n}_1}{\bar{n}_2+1} \right]^{1/2} (n_2-\bar{n}_2) \\ & - \frac{\lambda}{4} \left[\left[\frac{\bar{n}_2+1}{\bar{n}_1^{\,3}} \right]^{1/2} (n_1-\bar{n}_1)^2 + \left[\frac{\bar{n}_1}{(\bar{n}_2+1)^3} \right]^{1/2} (n_2-\bar{n}_2)^2 \right. \\ & \left. - [\bar{n}_1(\bar{n}_2+1)]^{-1/2} (n_1-\bar{n}_1)(n_2-\bar{n}_2) + \cdots \right] . \end{aligned} \tag{3.10}$$

Retaining terms up to first order we have

$$\begin{aligned} W(t) = -\mathrm{Re}\left\{ e^{2i\lambda \pm [\bar{n}_1(\bar{n}_2+1)]^{1/2}} \sum_{n_1=0}^{\infty} \sum_{n_2=0}^{\infty} P_{n_1}(\bar{n}_1) P_{n_2}(\bar{n}_2) \exp\left[i\lambda t \left[\frac{\bar{n}_2+1}{\bar{n}_1} \right]^{1/2} (n_1-\bar{n}_1) \right] \right. \\ \left. \times \exp\left[i\lambda t \left[\frac{\bar{n}_1}{\bar{n}_2+1} \right]^{1/2} (n_2-\bar{n}_2) \right] \right\} . \end{aligned} \tag{3.11}$$

The initial factor gives the rapid Rabi oscillation at $\Omega(\bar{n}_1, \bar{n}_2)$ and the oscillating exponential terms in the sum determine the revivals. These will occur at times when the two oscillations are in phase, which happens when the following conditions are satisfied:

$$\begin{aligned} \lambda t_R \left[\frac{\bar{n}_2+1}{\bar{n}_1} \right]^{1/2} &= 2\pi k, \quad k = 0,1,2,\ldots , \\ \lambda t_R \left[\frac{\bar{n}_1}{\bar{n}_2+1} \right]^{1/2} &= 2\pi l, \quad l = 0,1,2,\ldots . \end{aligned} \tag{3.12}$$

By multiplying these two equations together we obtain simply $(\lambda t_R)^2 = 4\pi^2 kl$, or

$$\lambda t_R = 2\pi\sqrt{m}, \quad m = kl = 0,1,2,\ldots . \tag{3.13}$$

On the other hand, by dividing the two Eqs. (3.12) we arrive at

$$\frac{\bar{n}_2+1}{\bar{n}_1} = \frac{k}{l} . \tag{3.14}$$

Now Eq. (3.13) alone, for $m = 1,2,3$, etc., predicts a sequence of revivals at 2π, 8.89, 10.88, 4π, 14.05, etc., which in fact does agree well with the observed locations of revivals in Fig. 3. Interestingly, the graphs do not always show revivals at the times predicted by Eq. (3.13), but when a revival occurs, it occurs at one of those times. The puzzle is that Eq. (3.14) should also be satisfied, which is clearly not possible for all the various k and l used to generate the revival times in Eq. (3.13). It should also be pointed out that these predictions are also valid for a Jaynes-Cummings model involving the related two-photon two-mode interaction of the form $\sigma_+ a_1 a_2 + \mathrm{H.c.}$ recently studied by Gou.[17] Indeed, the positions of revivals exhibited (without comment) by Gou show the same behavior.

IV. FIELD STATISTICS

We now study the dynamics of the field statistics of our system, paying particular attention to the production of states of the field exhibiting nonclassical properties. In particular, we examine the possible production of antibunched light, anticorrelations between the two modes, violations of the Cauchy-Schwartz inequality, and the appearance of squeezing in each mode.

But first, let us consider the time evolution of the average photon number in each of the modes. From Eq. (2.21b), the two-mode photon number distribution function $P_{n_1 n_2}(\bar{n}_1, \bar{n}_2, t)$ is

$$P_{n_1 n_2}(\bar{n}_1,\bar{n}_2,t)=\rho_I^F\begin{Bmatrix} n_1 & n_1 \\ n_2 & n_2 \end{Bmatrix}(t)$$
$$=P_{n_1}(\bar{n}_1)P_{n_2}(\bar{n}_2)\cos^2\{\lambda t[n_1(n_2+1)]^{1/2}\}+P_{n_1+1}(\bar{n}_1)P_{n_2-1}(\bar{n}_2)\sin^2\{\lambda t[n_2(n_1+1)]^{1/2}\}\ , \tag{4.1}$$

from which the average photon numbers $\bar{n}_1(t)$, $\bar{n}_2(t)$ are obtained as

$$\bar{n}_1(t)=\sum_{n_1=0}^{\infty}\sum_{n_2=0}^{\infty} n_1 P_{n_1 n_2}(\bar{n}_1,\bar{n}_2,t)\ , \tag{4.2a}$$

$$\bar{n}_2(t)=\sum_{n_1=0}^{\infty}\sum_{n_2=0}^{\infty} n_2 P_{n_1 n_2}(\bar{n}_1,\bar{n}_2,t)\ , \tag{4.2b}$$

and where $\bar{n}_1(0)\equiv\bar{n}_1$, $\bar{n}_2(0)\equiv\bar{n}_2$. In the special case when $\bar{n}_1\neq 0$, $\bar{n}_2=0$, these become

$$\bar{n}_1(t)=\frac{1}{2}\left[\bar{n}_1+\sum_{n_1=0}^{\infty} n_1 P_{n_1}(\bar{n}_1)\cos[2\lambda t(n_1)^{1/2}]\right]\ , \tag{4.3a}$$

$$\bar{n}_2(t)=\frac{1}{2}\left[\bar{n}_1\overline{\left[\frac{1}{n_1+1}\right]}-\bar{n}_1\sum_{n_1=0}^{\infty}\left[\frac{1}{n_1+1}\right]P_{n_1}(n_1)\times\cos[2\lambda t(n_1+1)^{1/2}]\right] \tag{4.3b}$$

where it should be noted that $\bar{n}_1=\sum_{n_1=0}^{\infty} n_1 P_{n_1}(\bar{n}_1)$, $\bar{n}_2=\sum_{n_2=0}^{\infty} n_2 P_{n_2}(\bar{n}_2)$, and that

$$\sum_{n_1=0}^{\infty} P_{n_1+1}(\bar{n}_1)=\bar{n}_1\sum_{n_1=0}^{\infty}\left[\frac{1}{n_1+1}\right]P_{n_1}(\bar{n}_1)$$
$$=\bar{n}_1\overline{\left[\frac{1}{n_1+1}\right]}\ . \tag{4.4}$$

The oscillations of the average photon numbers are clearly related to the Rabi oscillations as seen in the atomic inversion. The dominant frequency of the Rabi oscillations is $\Omega(\bar{n}_1)=2\lambda(\bar{n}_1)^{1/2}$. In the second term of Eq. (4.3b), the function $P_{n_1+1}(\bar{n}_1)$ peaks at about $n_1+1\approx\bar{n}_1$ so that both $\bar{n}_1(t)$ and $\bar{n}_2(t)$ also oscillate at this frequency. In Fig. 4 we plot $\bar{n}_1(t)$ and $\bar{n}_2(t)$ versus the scaled time λt where it is clear that, as expected, these quantities exhibit the same pattern of collapse and revival as the atomic inversion.

In Fig. 5 we plot $\bar{n}_1(t)$ and $\bar{n}_2(t)$ for the case when $\bar{n}_1=10$, $\bar{n}_2=5$ and it is quite clear that in this case we also obtain the same pattern as for the atomic inversion.

We now turn to the problem of obtaining evidence of nonclassical properties of the light beams. We should point out that Bogolubov *et al.*[18,19] have studied the statistical properties of a three-level system in the configuration of Fig. 1, but without the adiabatic removal

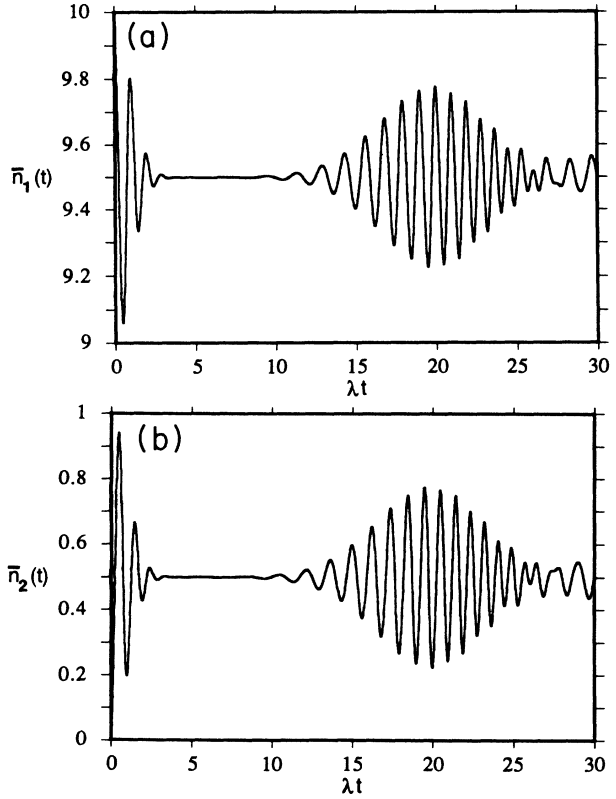

FIG. 4. For $\bar{n}_1=10$ and $\bar{n}_2=0$, (a) $\bar{n}_1(t)$ vs λt and (b) $\bar{n}_2(t)$ vs λt.

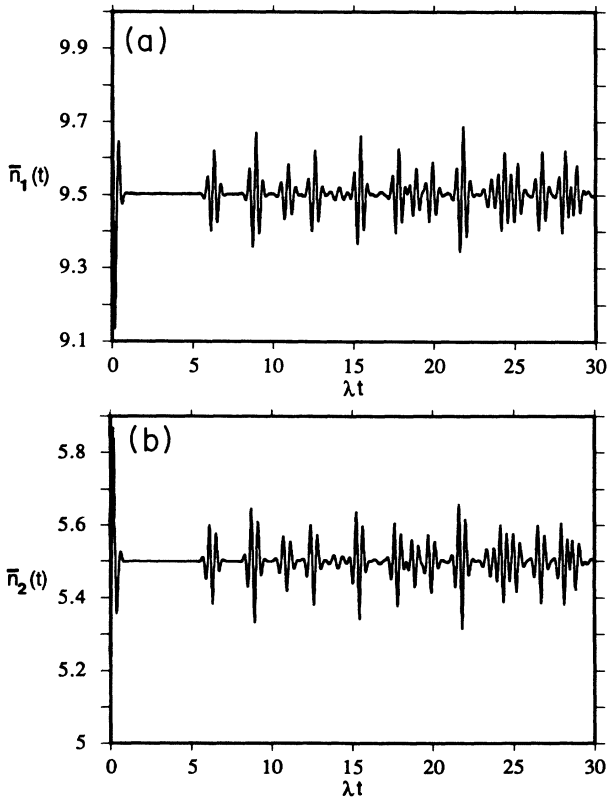

FIG. 5. For $\bar{n}_1=10$ and $\bar{n}_2=5$, (a) $\bar{n}_1(t)$ vs λt and (b) $\bar{n}_2(t)$ vs λt.

of the second level. In their work, evidence of strong nonclassical properties was found and similar behavior is expected in the present study.

To characterize the statistical properties of the light beams, we introduce the function[20]

$$\gamma_{ij}^{(2)}=\frac{\langle a_i^\dagger a_j^\dagger a_j a_i\rangle}{\langle a_i^\dagger a_i\rangle\langle a_j^\dagger a_j\rangle},\quad i,j=1,2\ . \tag{4.5}$$

Here $\gamma_{ii}^{(2)}$ defines the degrees of second-order coherence in the modes and $\gamma_{12}^{(2)}$ describes the degree of intermode correlation.

We first consider the second-order coherence of the modes. The function $\gamma_{ii}^{(2)}$ can be written in terms of the normally ordered photon number variance $\langle :(\Delta N_i)^2:\rangle$ as

$$\gamma_{ii}^{(2)}=1+\frac{\langle :(\Delta N_i)^2:\rangle}{\langle N_i\rangle^2} \tag{4.6}$$

where $N_i=a_i^\dagger a_i$ and

$$\langle :(\Delta N_i)^2:\rangle=\langle a_i^\dagger a_i^\dagger a_i a_i\rangle-\langle N_i\rangle^2\ . \tag{4.7}$$

The light is nonclassical, exhibiting the sub-Poisson statistics, whenever $\gamma_{ii}^{(2)}<1$ or equivalently whenever $\langle :(\Delta N_i)^2:\rangle<0$. Since we are actually calculating the zero time delay coherence function, states satisfying these conditions are more properly referred to as antibunched. The expectation values $\langle N_i(t)\rangle=\bar{n}_i(t)$ are just those given by Eq. (4.2) while the first term of the right of Eq. (4.7) is given by

$$\langle a_i^\dagger(t)a_i^\dagger(t)a_i(t)a_i(t)\rangle=\sum_{n_1=0}^{\infty}\sum_{n_2=0}^{\infty}n_i(n_i-1)P_{n_1n_2}(\bar{n}_1,\bar{n}_2,t)\ . \tag{4.8}$$

For the special case $\bar{n}_1\neq 0$, $\bar{n}_2=0$ we obtain

$$\langle a_1^\dagger(t)a_1^\dagger(t)a_1(t)a_1(t)\rangle=\frac{1}{2}\left[\bar{n}_1^{\,2}+\sum_{n_1=0}^{\infty}n_1(n_1-1)P_{n_1}(\bar{n}_1)\cos[2\lambda t(n_1)^{1/2}]\right], \tag{4.9}$$

$$\langle a_2^\dagger(t)a_2^\dagger(t)a_2(t)a_2(t)\rangle=0 \tag{4.10}$$

where $\bar{n}_1^{\,2}$ is just the expectation value of $\langle a_1^\dagger a_1^\dagger a_1 a_1\rangle$ with the coherent state $|\alpha_1\rangle$ at $t=0$. Thus we have

$$\langle :[\Delta N_1(t)]^2:\rangle=\frac{1}{2}\left[\sum_{n_1=0}^{\infty}n_1(n_1-1)P_{n_1}(\bar{n}_1)\cos[2\lambda t(n_1)^{1/2}]-\bar{n}_1^{\,2}(t)\right], \tag{4.11}$$

$$\langle :[\Delta N_1(t)]^2:\rangle=-\bar{n}_2^{\,2}(t)\ . \tag{4.12}$$

It appears that for this special case, sub-Poisson statistics will always be present in the second mode. This result agrees with the prediction of Bogolubov *et al.*,[18] obtained by retaining the excited state. In Fig. 6 we plot the normally ordered variances for both modes with $\bar{n}_1=10$, $\bar{n}_2=0$. We notice that mode 1 shows antibunching only for short time periods. The collapse and revival patterns of course are the same as for the atomic inversion.

In Fig. 7, we plot the normally ordered variances of the photon number operators for the case when $\bar{n}_1=10$, $\bar{n}_2=5$. No antibunching is observed in the first mode but dominates the second mode.

Also of interest is the degree of interbeam second-order coherence determined by

$$\gamma_{12}^{(2)}=\frac{\langle a_1^\dagger a_2^\dagger a_2 a_1\rangle}{\langle a_1^\dagger a_1\rangle\langle a_2^\dagger a_2\rangle}\ . \tag{4.13}$$

We actually calculate the cross-correlation function (or the covariance of the product of the photon number operators) between the two modes as defined by

$$C(t)=\langle a_1^\dagger(t)a_2^\dagger(t)a_2(t)a_1(t)\rangle-\langle a_1^\dagger(t)a_1(t)\rangle\langle a_2^\dagger(t)a_2(t)\rangle\ , \tag{4.14}$$

which is proportional to the excess coincidence counting rate for a Hanbury-Brown-Twiss-type experiment with

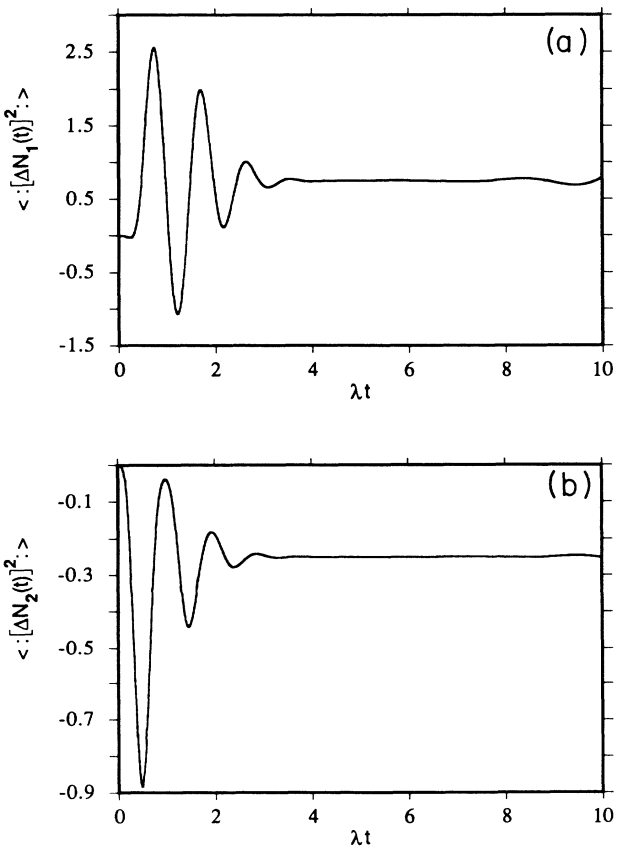

FIG. 6. For $\bar{n}_1=10$ and $\bar{n}_2=0$, (a) $\langle :[\Delta N_1(t)]^2:\rangle$ vs λt, (b) $\langle :[\Delta N_2(t)]^2:\rangle$ vs λt.

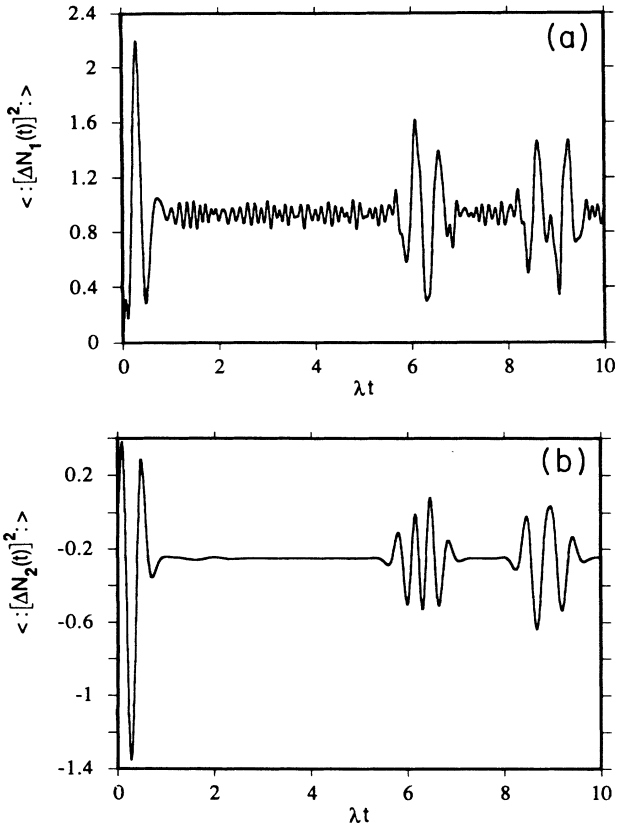

FIG. 7. For $\bar{n}_1=10$ and $\bar{n}_2=5$, (a) $\langle:[\Delta N_1(t)]^2:\rangle$ vs λt, (b) $\langle:[\Delta N_2(t)]^2:\rangle$ vs λt.

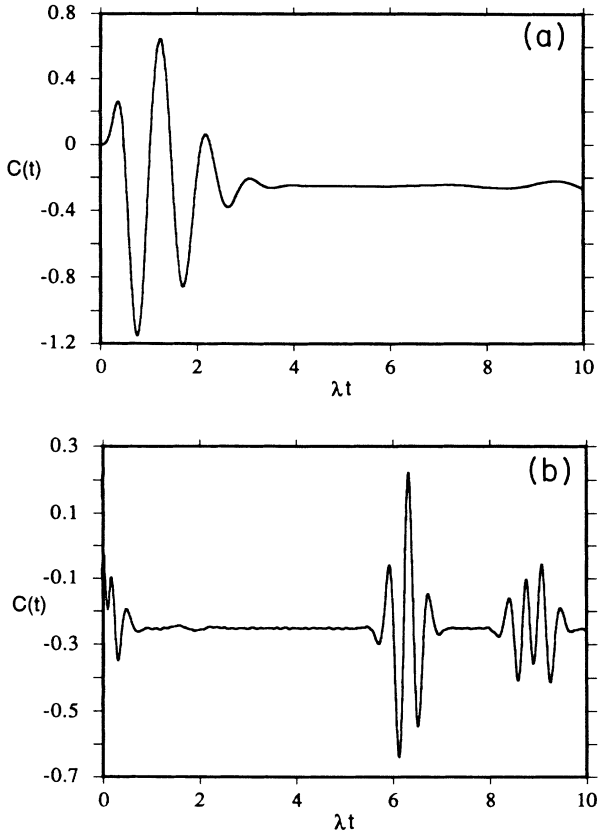

FIG. 8. Cross-correlation function $C(t)$ vs λt for (a) $\bar{n}_1=10$, $\bar{n}_2=0$, (b) $\bar{n}_1=10$, $\bar{n}_2=5$.

two beams,[21] where

$$\langle a_1^\dagger(t)a_2^\dagger(t)a_2(t)a_1(t)\rangle=\sum_{n_1=0}^{\infty}\sum_{n_2=0}^{\infty}n_1n_2P_{n_1n_2}(\bar{n}_1,\bar{n}_2,t)\ . \tag{4.15}$$

For $C(t)=0$ the beams are uncorrelated ($\gamma_{12}^{(2)}=0$), for $C(t)>0$ they are correlated ($\gamma_{12}^{(2)}>0$), and for $C(t)<0$ they are anticorrelated ($\gamma_{12}^{(2)}<0$). Because of the nature of the interaction in our model, where one photon is subtracted from one mode and added to the other, we expect the two modes to be predominantly anticorrelated. This is evident in Figs. 8(a) and 8(b) where we plot $C(t)$ versus λt for the cases $\bar{n}_1=10$, $\bar{n}_2=0$, and $\bar{n}_1=10$ and $\bar{n}_2=5$, respectively.

Finally in this vein, we consider the Cauchy-Schwartz inequality

$$(\gamma_{12}^{(2)})^2\le\gamma_{11}^{(2)}\gamma_{22}^{(2)} \tag{4.16}$$

which is violated by nonclassical states, indicating a nonclassical correlation between the beams. We actually calculate the quantity

$$\begin{aligned}V(t)=&\langle a_1^\dagger(t)a_2^\dagger(t)a_2(t)a_1(t)\rangle^2\\&-\langle a_1^\dagger(t)a_1^\dagger(t)a_1(t)a_1(t)\rangle\\&\times\langle a_2^\dagger(t)a_2^\dagger(t)a_2(t)a_2(t)\rangle\ .\end{aligned} \tag{4.17}$$

Whenever $V(t)$ is positive, the inequality in Eq. (4.16) is violated. For the special case when $\bar{n}_1\neq0$, $\bar{n}_2=0$, according to Eq. (4.10), $V(t)$ reduces to

$$V(t)=\langle a_1^\dagger(t)a_2^\dagger(t)a_2(t)a_1(t)\rangle^2>0\ , \tag{4.18}$$

where

$$\langle a_1^\dagger(t)a_2^\dagger(t)a_2(t)a_1(t)\rangle=\tfrac{1}{2}\bar{n}_1\left[\left[\frac{n_1}{n_1+1}\right]-\sum_{n_1=0}^{\infty}\left[\frac{n_1}{n_1+1}\right]P_{n_1}(\bar{n}_1)\cos[2\lambda t(n_1+1)^{1/2}]\right]\ , \tag{4.19}$$

so that apparently the inequality of Eq. (4.16) is always violated in this case. $V(t)$ versus λt for $\bar{n}_1=10$, $\bar{n}_2=0$ is plotted in Fig. 9(a). For $\bar{n}_2\neq0$, the inequality tends to be satisfied. For example, with $\bar{n}_1=10$, $\bar{n}_2=5$ [Fig. 9(b)], it is violated only for short time intervals and for $\bar{n}_1=10$, $\bar{n}_2=10$ [Fig. 9(c)] it appears not to be violated at all.

Finally in this section we consider the possible production of squeezed light in each of the two cavity modes.

First we introduce the field quadrature operators. The field in the Schrödinger picture has the form

$$\mathcal{E}(z)=\tfrac{1}{2}\sum_{i=1}^{2}\mathcal{E}_i(z)(a_i+a_i^\dagger) \tag{4.20}$$

where $\mathcal{E}_i(z)$ depends only on the cavity dimensions and mode frequencies and z is the direction of propagation. (The one-half factor is for convenience). The time-dependent quadrature operators $X_1^{(i)}(t)$ and $X_2^{(i)}(t)$ are introduced by writing the field as

$$\mathcal{E}(z)=\sum_{i=1}^{2}\mathcal{E}_i(z)[X_1^{(i)}(t)\cos(\omega_i t)+X_2^{(i)}(t)\sin(\omega_i t)] \ . \tag{4.21}$$

By comparing Eqs. (4.20) and (4.21) we obtain

$$X_1^{(i)}(t)=\tfrac{1}{2}(a_i e^{i\omega_i t}+a_i^\dagger e^{-i\omega_i t}) \ ,$$

$$X_2^{(i)}(t)=-\frac{i}{2}(a_i e^{i\omega_i t}-a_i^\dagger e^{-i\omega_i t}) \ . \tag{4.22}$$

These operators satisfy the commutation relations

$$[X_1^{(i)}(t),X_2^{(j)}(t)]=\frac{i}{2}\delta_{ij} \ , \tag{4.23}$$

which implies the uncertainty relations

$$\langle(\Delta X_1^{(i)})^2\rangle\langle(\Delta X_2^{(i)})^2\rangle\geq\tfrac{1}{16} \ . \tag{4.24}$$

Squeezing is said to exist whenever $\langle(\Delta X_j^{(i)})^2\rangle<\frac{1}{4}$ $(i,j=1,2)$.

In calculating the expectation values of the $X_j^{(i)}(t)$ and their squares, the rapid time oscillations at frequencies ω_1 and ω_2 are removed by the transformation of Eq. (2.13) so that in the interaction picture, the quadrature operators are just those of Eq. (4.22) but with $t=0$. In our calculations, we find it convenient to characterize the squeezing through the use of the Q parameter of Mandel[22] given by

$$Q_j^{(i)}=\frac{\langle(\Delta X_j^{(i)})^2\rangle-0.25}{0.25} \tag{4.25}$$

where $-1\leq Q_j^{(i)}<0$ for squeezing.

We have found that this model does not give rise to significant squeezing. We shall display only two examples of squeezing, both occurring in the quadrature $X_1^{(2)}$ and with the assumption that α_1 and α_2 are real. In Fig. 10(a) we plot $Q_1^{(2)}(t)$ versus λt for $\bar{n}_1=10$ and $\bar{n}_2=5$, where a small amount of squeezing is observed; about 20% below the vacuum noise level. For much higher initial average photon numbers $\bar{n}_1=100$ and $\bar{n}_2=50$, we see in Fig. 10(b) that $Q_1^{(2)}(t)$ does dip to about 10% below the vacuum level, after some initial rapid oscillations containing only miniscule squeezing.

The magnitude of the squeezing obtained in these cases is about the same as obtained in the usual one-photon Jaynes-Cummings model for low values of initial photon number. In that model, increasing the initial photon number apparently also increases the degree of squeezing obtained, contrary to the findings in the present case. The physical reason for the rather weak squeezing produced by this model is the fact that only one photon is absorbed or emitted from each mode. Squeezing is more efficiently produced in multiphoton processes such as degenerate or nondegenerate parametric amplification.[23] In fact, it has been demonstrated that the single-mode two-photon Jaynes-Cummings model can produce a greater degree of squeezing than the one-photon model.[10,11] Furthermore, recently Gou[17] has shown in the two-mode Jaynes-Cummings model that squeezing to about 40% below the vacuum level can be obtained in the superposition mode

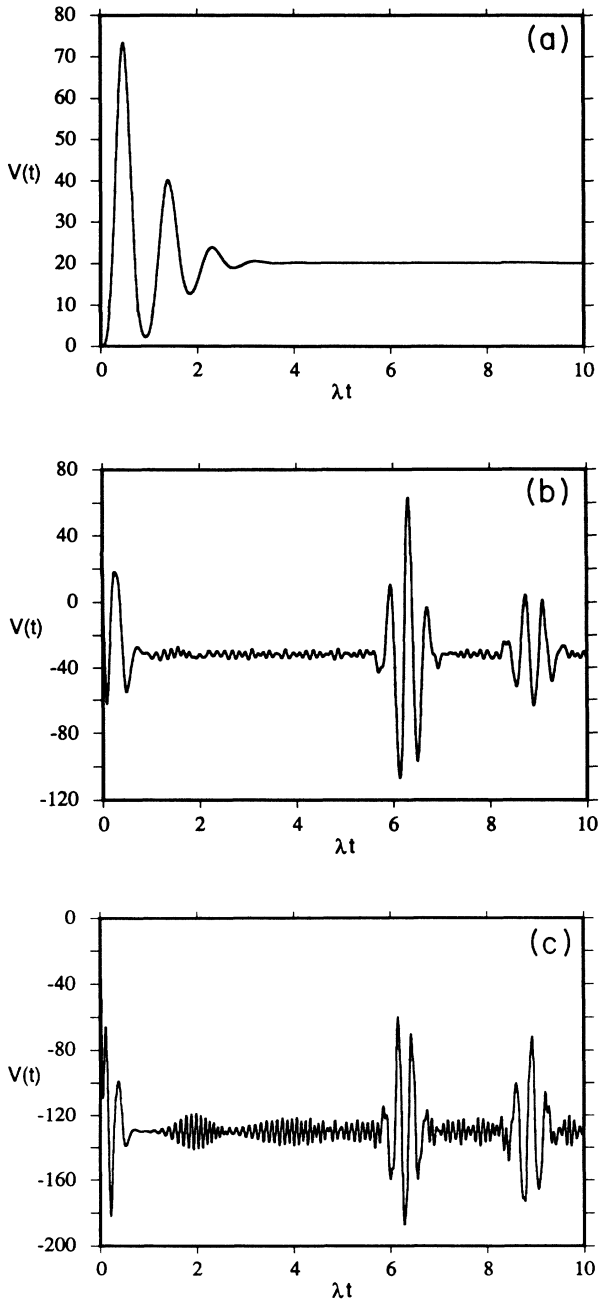

FIG. 9. $V(t)$ vs λt for (a) $\bar{n}_1=10$, $\bar{n}_2=0$, (b) $\bar{n}_1=10$, $\bar{n}_2=5$, (c) $\bar{n}_1=10$, $\bar{n}_2=10$.

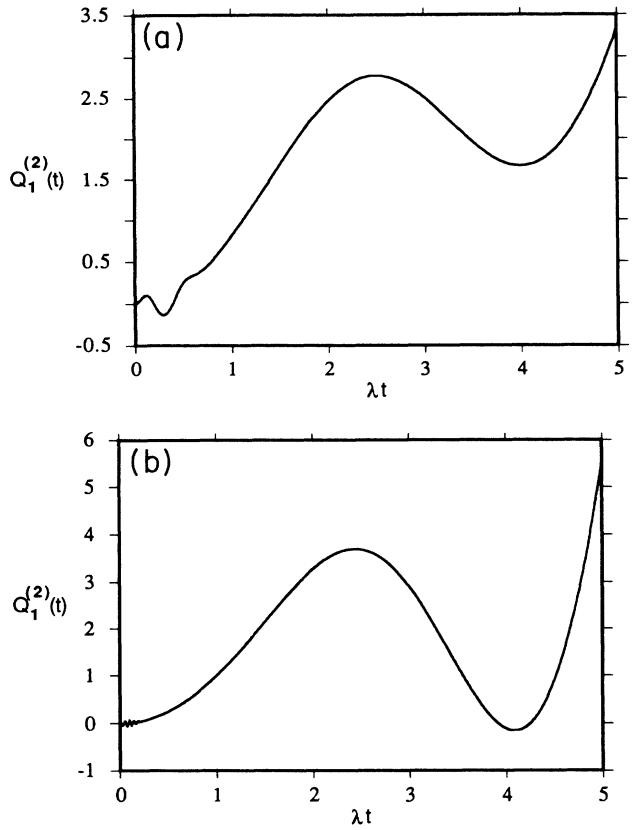

FIG. 10. $Q_1^{(2)}(t)$ vs λt for (a) $\bar{n}_1=10$, $\bar{n}_2=5$, (b) $\bar{n}_1=100$, $\bar{n}_2=50$.

quadratures of Caves and Schumaker.[24] We have studied these superposition mode quadratures for the present model and have not found squeezing even to the degree shown in Fig. 9.

V. SUMMARY AND DISCUSSION

In this paper, we have studied the quantum dynamics of a three-level atom in the Λ configuration interacting with two modes of the quantized electromagnetic field, with the upper level of the atom being effectively removed because it is far off resonance with both field modes. This two-mode Raman coupled system constitutes a cavity QED model of Raman scattering involving only the pump and Stokes modes (or only the pump and anti-Stokes) and as such is an example of a zero-photon process. It is another Jaynes-Cummings-like model that is fully quantized and exactly solvable.

As we have shown, it also admits many of the features of the usual Jaynes-Cummings model such as the collapse and revival of the Rabi oscillations and the production of nonclassical light. However, an unexpected feature is that the locations of the revivals in the time record of the coherent-state Rabi oscillations can be independent of the initial average photon numbers $\bar{n}_1$ and $\bar{n}_2$. This is still imperfectly explained.

The model has been shown to be effective in the production of some forms of nonclassical light. For example, if the Stokes mode is initially in the vacuum state, the light field generated in that mode is always antibunched, and the Cauchy-Schwartz inequality is always violated. We also find a strong tendency for the two modes to be anticorrelated, which is expected given the form of the interaction. Also, again on the basis of the form of the interaction, we do not expect this system to produce squeezed light effectively, and the numerical calculations apparently confirm this even at higher proton number.

Possible extensions of the present work are to study, for example, the effects of cavity damping on the quantum dynamics and the analog of the vacuum-field Rabi oscillations and time-dependent spectra. It would also be of interest to study the effects of driving the system with initially nonclassical fields, for example, squeezed states in one or both modes, or by field states containing correlations (or anticorrelations) between the modes. These matters are currently under consideration and results will be reported later.

ACKNOWLEDGMENTS

This work was partially supported by a grant from the National Science Foundation. We thank Dr. Rainer Grobe for many useful discussions and for assistance with the numerical calculations.

APPENDIX

In this Appendix we derive the effective interaction Hamiltonian Eq. (2.1) for the Raman coupled model of Fig. 1 under the assumption of large detuning.

Using the Hamiltonian of Eq. (2.4), the Heisenberg equations for the transition operators σ_{12} and σ_{23} are

$$i\dot{\sigma}_{12}=\frac{1}{\hbar}(E_2-E_1)\sigma_{12}+g_{12}a_1(\sigma_{11}-\sigma_{22})+g_{23}\sigma_{13}\ , \quad \text{(A1)}$$

$$i\dot{\sigma}_{23}=-\frac{1}{\hbar}(E_2-E_3)\sigma_{23}-g_{12}a_1^{\dagger}\sigma_{13}+g_{23}a_2^{\dagger}(\sigma_{22}-\sigma_{33})\ . \quad \text{(A2)}$$

We now introduce the "slow" variables (denoted with the tilde)

$$\sigma_{12}=\tilde{\sigma}_{12}e^{-i\omega_1 t},\quad \sigma_{23}=\tilde{\sigma}_{23}e^{i\omega_2 t},$$
$$a_1=\tilde{a}_1 e^{-i\omega_1 t},\quad a_2=\tilde{a}_2 e^{-i\omega_2 t}. \quad \text{(A3)}$$

Also we introduce

$$\sigma_{13}=\sigma_{12}\sigma_{23}=\tilde{\sigma}_{12}\tilde{\sigma}_{23}e^{-i(\omega_1-\omega_2)t}$$
$$=\tilde{\sigma}_{13}e^{-i(\omega_1-\omega_2)t} \quad \text{(A4)}$$

where $\tilde{\sigma}_{13}=\tilde{\sigma}_{12}\tilde{\sigma}_{23}$. Substituting Eqs. (A3) and (A4) into Eqs. (A1) and (A2) we obtain

$$i\dot{\sigma}_{12}=\Delta\tilde{\sigma}_{12}+g_{12}\tilde{a}_1(\sigma_{11}-\sigma_{22})+g_{23}\tilde{a}_2\tilde{\sigma}_{13}\ , \quad \text{(A5)}$$

$$i\dot{\sigma}_{23}=-\Delta\tilde{\sigma}_{23}-g_{12}\tilde{a}_1^{\dagger}\tilde{\sigma}_{13}+g_{23}\tilde{a}_2^{\dagger}(\sigma_{22}-\sigma_{33}) \quad \text{(A6)}$$

which Δ is defined in Eq. (2.3). The "adiabatic" solutions, obtained in the limit when Δ is sufficiently large, are

$$\tilde{\sigma}_{12}=-\frac{1}{\Delta}[g_{12}\tilde{a}_1(\sigma_{11}-\sigma_{22})+g_{23}\tilde{a}_2\tilde{\sigma}_{13}] , \quad \text{(A7)}$$

$$\tilde{\sigma}_{23}=\frac{1}{\Delta}[-g_{12}\tilde{a}_1^{\dagger}\tilde{\sigma}_{13}+g_{23}\tilde{a}_2^{\dagger}(\sigma_{22}-\sigma_{33})] . \quad \text{(A8)}$$

After restoring the rapidly oscillating time dependence we have

$$\sigma_{12}=-\frac{1}{\Delta}[g_{12}a_1(\sigma_{11}-\sigma_{22})+g_{23}a_2\sigma_{13}] , \quad \text{(A9)}$$

$$\sigma_{23}=\frac{1}{\Delta}[-g_{12}a_1^{\dagger}\sigma_{13}+g_{23}a_2^{\dagger}(\sigma_{22}-\sigma_{33})] . \quad \text{(A10)}$$

Now the terms diagonal in the atomic variables will lead to Stark shifts which we shall assume to be small. By dropping these terms we obtain

$$\sigma_{12}\simeq-\frac{1}{\Delta}g_{23}a_2\sigma_{13} , \quad \text{(A11)}$$

$$\sigma_{23}\simeq-\frac{1}{\Delta}g_{12}a_1^{\dagger}\sigma_{13} . \quad \text{(A12)}$$

Upon inserting these results in Eq. (2.2b) we arrive at the effective interaction Hamiltonian

$$H_{I,\text{eff}}=-\hbar\lambda(\sigma_+a_1a_2^{\dagger}+\sigma_-a_1^{\dagger}a_2) \quad \text{(A13)}$$

where $\lambda=2(g_{12}g_{23})/\Delta$, and where we have set $\sigma_+=\sigma_{31}$ and $\sigma_-=\sigma_{13}$.

*Permanent address: Department of Physics, St. Bonaventure University, St. Bonaventure, NY 14778.

[1]For a review and many references, see H.-I. Yoo and J. H. Eberly, Phys. Rep. **118**, 239 (1985).

[2]For experimental work see Y. Kaluzny, P. Goy, M. Gross, R. M. Raimond, and S. Haroche, Phys. Rev. Lett. **51**, 1175 (1983); G. Rempe, H. Walther, and N. Klein, *ibid.* **58**, 353 (1987); M. G. Raizen, R. J. Thompson, R. J. Brecha, H. J. Kimble, and H. J. Carmichael, *ibid.* **63**, 240 (1989); Yifu Zhu, D. J. Gauthier, S. E. Morin, Q. Wu, H. J. Carmichael, and T. W. Mossberg, *ibid.* **64**, 2499 (1990); and G. Rempe, H. Walther, and F. Schmidt-Kaler, *ibid.* **64**, 2783 (1990).

[3]E. T. Jaynes and F. W. Cummings, Proc. IEEE **51**, 89 (1962).

[4]J. H. Eberly, N. B. Narozhny, and J. J. Sanchez-Mondragon, Phys. Rev. Lett. **44**, 1323 (1980); N. B. Narozhny, J. J. Sanchez-Mondragon, and J. H. Eberly, Phys. Rev. A **23**, 236 (1981).

[5]J. J. Sanchez-Mondragon, N. B. Narozhny, and J. H. Eberly, Phys. Rev. Lett. **51**, 550 (1983).

[6]P. Meystre and M. S. Zubairy, Phys. Lett. **89A**, 390 (1982); P. Filipowicz, J. Javanainen, and P. Meystre, J. Opt. Soc. Am. B **3**, 906 (1986).

[7]B. Buck and C. V. Sukumar, Phys. Lett. **81A**, 132 (1981); C. V. Sukumar and B. Buck, *ibid.*, **83A**, 211 (1981).

[8]S. Singh, Phys. Rev. A **35**, 3206 (1982).

[9]R. R. Puri and G. S. Agarwal, Phys. Rev. A **37**, 3879 (1988); R. R. Puri and R. K. Bullough, J. Opt. Soc. Am. B **5**, 2021 (1988).

[10]C. C. Gerry, Phys. Rev. A **37**, 2683 (1988); C. C. Gerry and P. J. Moyer, *ibid.* A **38**, 5665 (1988).

[11]A. S. Shumovsky, F. Le Kien, and E. I. Aliskenderov, Phys. Lett. A **124**, 351 (1988).

[12]See D. Meschede, H. Walther, and G. Müller, Phys. Rev. Lett. **54**, 551 (1984); M. Brune, J. M. Raimond, P. Goy, L. Davidovich, and S. Haroche, *ibid.* **59**, 1899 (1987).

[13]See, for example, N. N. Bogolubov, Jr., F. Le Kien, and A. S. Shumovsky, J. Phys. A **19**, 191 (1986); X.-S. Li and Y.-N. Peng, Phys. Rev. A **32**, 1501 (1985); S.-Y. Zhu, J. Mod. Opt. **36**, 499 (1989).

[14]S. Stenholm, Phys. Rep. **6**, 1 (1973).

[15]P. L. Knight, Phys. Scr. **T12**, 51 (1986).

[16]S. J. D. Phoenix and P. L. Knight, J. Opt. Soc. Am. B **7**, 116 (1990).

[17]S.-C. Gou, Phys. Rev. A **40**, 5116 (1989).

[18]N. N. Bogolubov, Jr., F. Le Kien, and A. S. Shumovsky, J. Phys. (Paris) **47**, 427 (1986).

[19]N. N. Bogolubov, Jr., F. Le Kien, and A. S. Shumovsky, Europhys. Lett. **4**, 281 (1987).

[20]R. Loudon, Rep. Prog. Phys. **43**, 58 (1979).

[21]H. Paul, Rev. Mod. Phys. Phys. **58**, 209 (1986).

[22]L. Mandel, Phys. Rev. Lett. **47**, 709 (1981).

[23]See the review, R. Loudon and P. L. Knight, J. Mod. Opt. **34**, 709 (1987).

[24]C. M. Caves and B. L. Schumaker, Phys. Rev. A **31**, 3068 (1985); B. L. Schumaker and C. M. Caves, *ibid.* **31**, 3093 (1985).